ORIGINAL ARTICLE

Porous alumina ceramics by gel casting: Effect of type of sacrificial template on the properties

Saleh Hooshmand[1] | **Jan Nordin**[2] | **Farid Akhtar**[1] (iD)

[1]Division of Materials Science, Luleå University of Technology, Luleå, Sweden

[2]Akzo Nobel Pulp and Performance Chemicals AB, Expancel, Sundsvall, Sweden

Correspondence
Farid Akhtar, Division of Materials Science, Luleå University of Technology, Luleå 97187, Sweden.
Email: farid.akhtar@ltu.se

Abstract

The effect of type of sacrificial template on the processing and properties of porous alumina ceramics was investigated. Two templates, (a) hollow pre-expanded polymer spheres (Expancel) and (b) dense glassy carbon, were used to prepare porous alumina ceramics by gel casting. The results showed that the burnout of sacrificial expandable polymer microspheres from alumina ceramics was 10 times faster than glassy carbon without compromising the compressive strength. Moreover, the effect of the size of the porous ceramic component during the burnout showed that the template decomposition and the escape of the formed gases took a longer time for the thicker specimens than the thinner one and it was significant in case of glassy carbon. It was found that the burnout of expandable microspheres could happen at a faster rate, and the time of the burnout cycle could be reduced significantly to save energy while keeping the mechanical strength twice as high than porous alumina ceramics after burnout of glassy carbon. Furthermore, the CO_2 emissions during the burnout of sacrificial templates and the microstructure of the prepared porous alumina were compared for these two types of sacrificial templates. The prepared foams with pre-expanded microspheres showed potential for being used in industrial applications, where the decreasing of the released gases is critical for saving time and energy for the fabrication of large ceramic parts.

KEYWORDS

alumina, ceramic foam, gelcasting, mechanical properties, porous materials, sacrifical template

1 | INTRODUCTION

Ceramics offer advantages compared to other materials such as polymers and metals, such as hardness, chemical inertness, thermal shock resistance, corrosion, and wear resistance.[1–3] Addition of porosity to ceramics introduces low thermal mass, low thermal conductivity, controlled permeability, high surface area, low density, and high specific strength.[4] These added properties make the porous ceramics attractive to be used widely in various versatile applications like filters for diesel emissions, molten metal filters, high-temperature thermal insulation, membrane reactors, and catalyst supports.[4–7] Wet processing route in the processing of porous ceramic is promising compared to the dry processing route since it offers better control on particle-particle interactions and homogeneity of particles, which lead to fewer defects in the ceramic microstructure.[8,9] Gel casting is a wet processing method based on the sacrificial template technique, and it is widely used to prepare high-quality complex-shaped porous ceramic

parts with controlled morphologies, porosity, and properties.[9] It was first developed in 1990 in the Oak Ridge National Laboratory (ORNL),[10] and the principle is based on in situ polymerization of acrylamide monomers to form a 3D network gel to hold the suspended ceramic particles in the desired shape. The gelled part is dried in controlled conditions to form a mechanically stable green body, and subsequently, polymer burnout and sintering take place in a furnace at appropriate temperatures.[9] Gel casting is a generic process, which can be adapted for use with different ceramic types, ranging from alumina-based refractories to high-performance silicon nitride and silicon carbide for different applications.[11] Though gel casting is used widely to prepare small parts such as thin coatings and tapes, the larger gel-cast ceramic bodies often contain a large number of defects because of high internal stresses produced during the process of drying and volatile removal and burnout of the organic materials.[12] Gel-casted porous ceramics with tailored pore size can be prepared by addition of an appropriate amount of sacrificial template as the pore former. The template will be removed before or during the sintering process.[13] Different templates such as polymer beads, for example polymethylmethacrylate (PMMA)[14] and thermally expandable microspheres (Expancel),[15,16] potato starch,[17] graphite,[18] charcoal,[19] and paraffin wax[20] were found in the literature as the sacrificial template. Although the porosity of the final product is strongly influenced by the shape, size, and the amount of the template, the process of template removal has a significant effect on the properties. The removal of the organic templates can be time and energy demanding and might induce internal stress inside the ceramic body due to the high amount of gas release causing cracking and bubble formation.[16] Thus, decreasing the amount of released gases to avoid the formation of defects and decreasing the time for the template removal are critical for industrial use to prepare large ceramic parts.

The aim of this study is to investigate the effect of type of sacrificial template, (a) hollow expanded polymer spheres and (b) dense glassy carbon, to process porous alumina ceramics. The glassy carbon was chosen as the template since it is organic and was available with the spherical shape in different sizes. It has a relatively low density and has good mechanical properties, which cause no deformation during processing. Thus, both templates are organic with similar shape and size, which make the comparison more accurate. The effect of the use of hollow expanded polymer spheres and glassy carbon as sacrificial templates, during the drying and burnout cycle of the green bodies, on the mechanical stability is reported. The burnout cycle of porous alumina ceramics with expanded polymer spheres as a sacrificial template was optimized to achieve 10 times faster burnout cycles without compromising the compressive strength. Moreover, the effect of the size of

the porous ceramic component, furnace atmosphere, and CO_2 emissions during the burnout of sacrificial templates is discussed.

2 | EXPERIMENTAL

2.1 | Materials

High purity alumina powder (≥99.99 %), AKP-G15 (Sumitomo Chemical Co., Ltd., Tokyo, Japan), with γ crystalline structure and mean particle size of 0.6 μm and specific surface area of 3.5 m^2/g was used. Methacrylamide (MAM, $C_7H_{10}N_2O_2$,) and Methylenebisacrylamide (MBAM, $(C_2H_3CONH)_2CH_2$)) supplied by Sigma Aldrich, Germany, were used as monomers and cross-linker, respectively, to form the binder. Ammonium persulfate (APS, $H_8N_2O_8S_2$, Sigma Aldrich, Germany) as an initiator, sodium dodecyl sulfate (SDS, $C_{12}H_{25}NaO_4S$, Sigma Aldrich, Germany) as a surfactant, and "1-butanol" (C_4H_9OH, Merck, Germany) as an anti-foaming agent were used. Dry expanded polymeric spheres (Expancel Microspheres, AkzoNobel Pulp and Performance Chemicals AB, Sundsvall, Sweden) with the size of 20-40 μm and bulk density of 60 ± 5 kg/m^3 and glassy carbon spheres (SPI Supplies, West Chester, USA) with the size of 40-80 μm and density of 1400 kg/m^3 were used as sacrificial templates. Unlike the previous study in which wet Expancel was used,[15] in this study the dry Expancel was chosen, as the objective was to compare the EPS with the GC and since the GC has no water on its surface, using dry EPS keeps the condition the same for both templates.

2.2 | Gel casting of porous alumina ceramics

Three types of porous ceramic were prepared as follows: (a) alumina ceramics without a sacrificial template; (b) alumina ceramics with expanded polymer microspheres (EPS); and (c) alumina ceramics with glassy carbon (GC). Initially, the monomer (MAM) and cross-linker (MBAM) were mixed in ratio 5:1 in distilled water at 90°C for 2 minutes using a magnetic stirrer to form a 10 wt. % organic solution. Alumina powder was added gradually to reach around 36 vol.%. Afterward, the surfactant, SDS (1-1.5 wt. % of alumina), was added and mixed using magnetic stirrer for 6 minutes. The slurry was ball milled in a polyethylene bottle contained alumina milling beads for 24 hours. The ball-milled suspensions were degassed for 10 minutes using a vacuum pump, and 1 wt. % of an anti-foaming agent, 1-butanol was added. An appropriate amount of pore formers, EPS or GC, to reach 25 vol. % (1.5 wt. % for EPS and 35 wt. % for GC), and the initiator (APS) was added to the slurry and mixed using magnetic stirrer for 30 minutes, and then, the suspensions were cast in glass molds. The processing steps are shown in
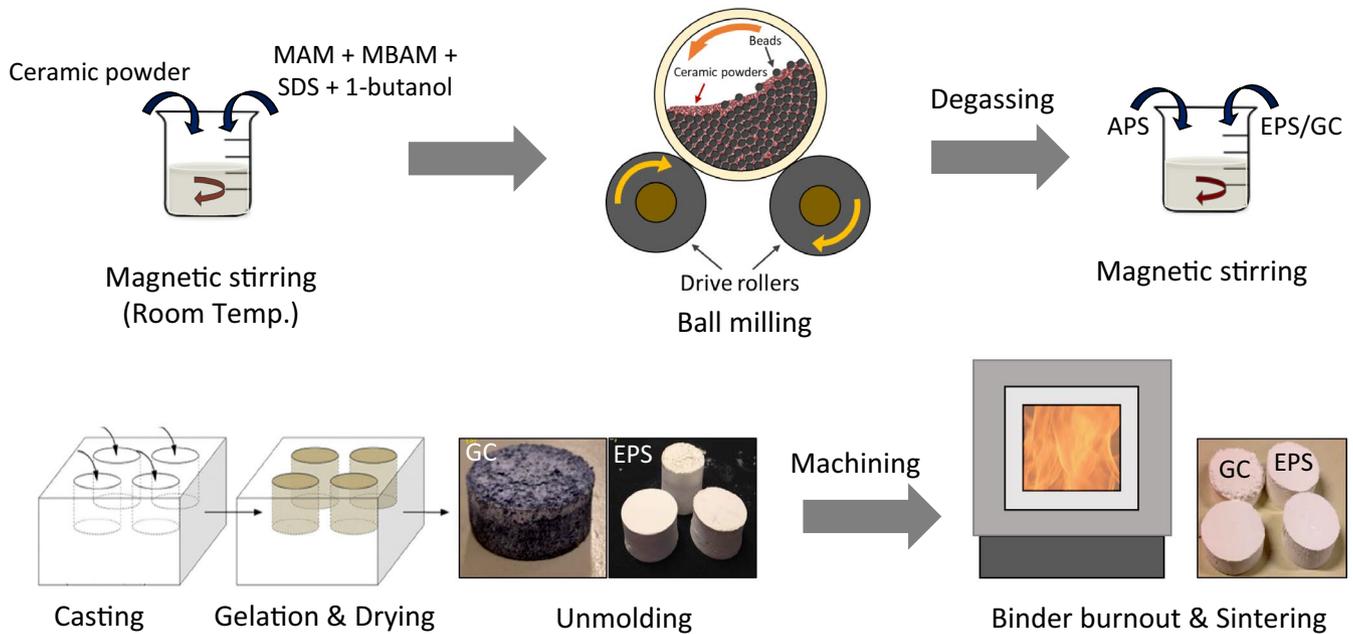
FIGURE 1 Schematic view of gel-casting process and specimens before and after burnout cycle

Figure 1 and have been explained more in detail by Ciurans Oset et al[15]. The properties of the molds play an important role in forming the green body, as it must allow shrinkage to occur and minimize stresses in the cast part during drying. To reduce the risk of crack formation during drying, the thermal expansion coefficient (CTE) of the mold should be as close as possible to one of the alumina. For this reason, glass mold (CTE = 5.9 10^{-6}/K) was used to cast alumina ceramic (CTE = 5.4 10^{-6}/K). The gel-cast bodies in the glass mold were placed in a preheated oven, first for 6 hours at 50°C at a relative humidity of 75 %. Then, the gel-cast bodies were removed from glass mold and kept for drying at room temperature for 3 days at a relative humidity of 75% followed by final drying at 115°C for 6 hours in the air to remove the remaining moisture. The dried green bodies were mechanically stable for machining, and specimens of size $10 \times 10 \times 10$ mm^3 were prepared to measure the compressive strength of the burned-out specimens. The organic components were removed (burned out) at 600°C under air at a heating rate of 1, 3, and 10°C/min to reach 600°C and held for 12 hours to complete the burnout step.

2.3 | Characterization

To study the weight loss and the shrinkage of the foams with and without the template, the weight and the upper diameter of the samples were measured every 5 hours during the drying process for two specimens for each sample and the average value was reported. The weight loss and radial shrinkage (ε_r) were determined with Equations (1) and (2),

respectively, where W_0 and D_0 are the starting weight and the upper diameter, and W_i and D_i correspond to the weight and the upper diameter of the specimen after each measurement.

$$\% \text{ weight loss} = \frac{W_0 - W_i}{W_0} \times 100 \quad (1)$$

$$\% \, \varepsilon_r = \frac{D_0 - D_i}{D_0} \times 100 \quad (2)$$

The porosity of the presintered bodies was calculating using water as immersion liquid. The porous body was dried at 120°C for 2 hours and then cooled to room temperature in a desiccator. The dry body was weighed and then evacuated and infiltrated with distilled water to fill the open pores. The water-filled porous ceramic was weighed, and the porosity was calculated.
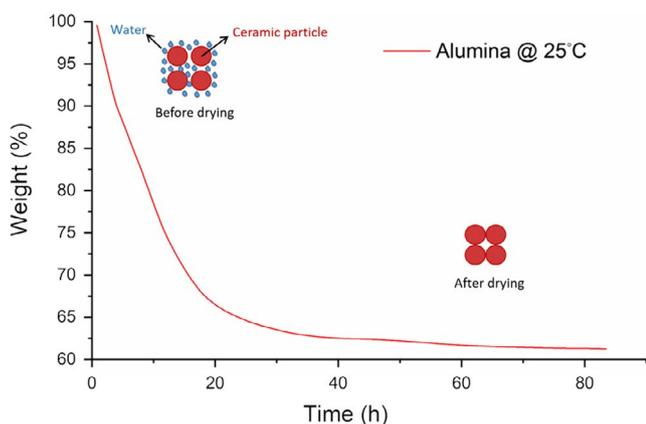
Thermogravimetric analysis (TGA) was performed using a simultaneous thermal analyzer (STA), Netzsch 414 Thermal Analyzer (Selb, Germany) coupled with a mass spectroscopy, in order to understand the template removal process and effect of furnace atmosphere on the burnout process. TGA was performed under air or argon atmosphere with a flow rate of 20 mL/min. Ceramic pellets with total weight 30 mg were used for the TGA studies. The buoyancy effect in TGA has been taken into account by carrying out empty crucible runs and subtracting the resulting weight differences from the subsequent sample mass loss data. The samples were heated to 1000°C with a heating rate of 10°C/min and cooled to room temperature with a cooling rate of 20°C/min. The microstructure of ceramic

bodies was studied using a scanning electron microscope (SEM), JEOL JSM-6460LV with the acceleration voltage of 10 kV. To study the mechanical properties of the samples after the template removal, an Instron 5967 universal testing machine (Instron 5967, Norwood, MA, USA) with 2 kN load cell and a crosshead speed of 0.5 mm/min were used. The compressive strength as a function of heating rate was measured, and an average value of three individual determinations for each sample was reported.

3 | RESULTS AND DISCUSSION

High solid loading is required to reduce the shrinkage of the ceramic green body during drying and sintering. The decrease in shrinkage reduces the problems of cracking and warping.[21] On the other hand, too high solid loading leads to high viscosity that is not suitable for mixing and casting. Flowable and stable porous alumina ceramics suspensions containing 36 vol.% alumina and 25 vol.% of expandable polymer spheres or glassy carbon as sacrificial template were gel-cast to produce green bodies following our previous work.[15] The gel-cast bodies were unmolded and kept at 25°C at a relative humidity of 25% for 85 hours. The weight loss during the drying of gel-cast alumina ceramics without pore formers is given in Figure 2.

It can be seen in Figure 2 that the variation of weight loss as a function of time involved two drying rates. First, from 0-20 hours, the drying rate is high and water evaporation occurs at the external surfaces of the ceramic body. And consequently, the distance between the particles decreases and the ceramic particles come in contact with each other and shrinkage of the ceramic body happens. The maximum drying shrinkage is reached at the end of the first stage. In the second stage, from about 40 hours of drying, the curve became flattered due to the low drying rate during the removal of internal water through the voids and pores between the particles, as well as through the cracks. At this stage, the weight loss occurs slowly as the removal of internal water needs a longer time. However, it should be noted that the binder together with some water remained in the structure between the ceramic particles. The drying shrinkage (DS) was anisotropic, which was higher in cross-section than the height of the cylindrical green body. The drying shrinkage for porous alumina sample without pore former was 20%, while for the samples consisting EPS and GC was 18% and 12%, respectively. The lower shrinkage of the specimens containing templates shows that the templates restricted the movements of the ceramic particles, during water evaporation. In case of GC, probably the higher density compared to EPS caused more restriction and consequently less shrinkage. The measured porosity of the presintered ceramic bodies with EPS and GC was 71% ± 2 and 69% ± 1, respectively, measured for three samples for each batch. The predicted porosity for each sample was 65%, based on random packing fraction of the powders (40% porosity) and the volume of the template, which was 25 vol.%. The higher measured porosity compared to the predicted values might be due to the binder burnout and the porosity originating from the trapped air bubbles.[15]

Figure 3 shows the weight loss vs temperature during the burnout process at a heating rate of 10°C. It can be seen that the burnout process is strongly affected by the furnace atmosphere. For the sample using EPS, under the inert argon atmosphere, the combustion could not start after the decomposition and the carbonyl groups remained inside the samples, and subsequently, the volatiles could not escape out, while in the presence of oxygen, templates were removed by thermal decomposition followed by combustion. Oxygen reacted with the carbonyl group and formed carbon dioxide and consequently completed the burnout process. It explains the higher weight decrease under oxygen compared to argon atmosphere (Figure 3A). For the sample with GC, as shown in Figure 3B, a significant decrease in weight can be observed after 600°C under the oxidative atmosphere, which is due to the combustion of the GC. This higher weight loss for GC compared to the EPS is due to the higher mass content of GC than EPS. The binder burnout should occur slowly to avoid bubble formation during the thermal decomposition of the polymers. Thus, it has been recommended to have a low heating rate to avoid the seal up of the external surface before the escape out of all the gases. In the case of high heating rate, the gases might be trapped inside the samples and expand during sintering which might cause bloating and consequently induces cracks.[22]

The microstructures of porous alumina ceramics before and after burnout of EPS and GC are shown in Figure 4. As SEM images reveal, in the green body (Figure 4A,C), the EPS and the GC are covered and surrounded by alumina powder. After the burnout of sacrificial templates, the pores appear and are distributed evenly, which shows good mixing prior to the gel formation during processing. Even though the

FIGURE 2 Weight loss vs time during drying of alumina ceramic without template at 25°C
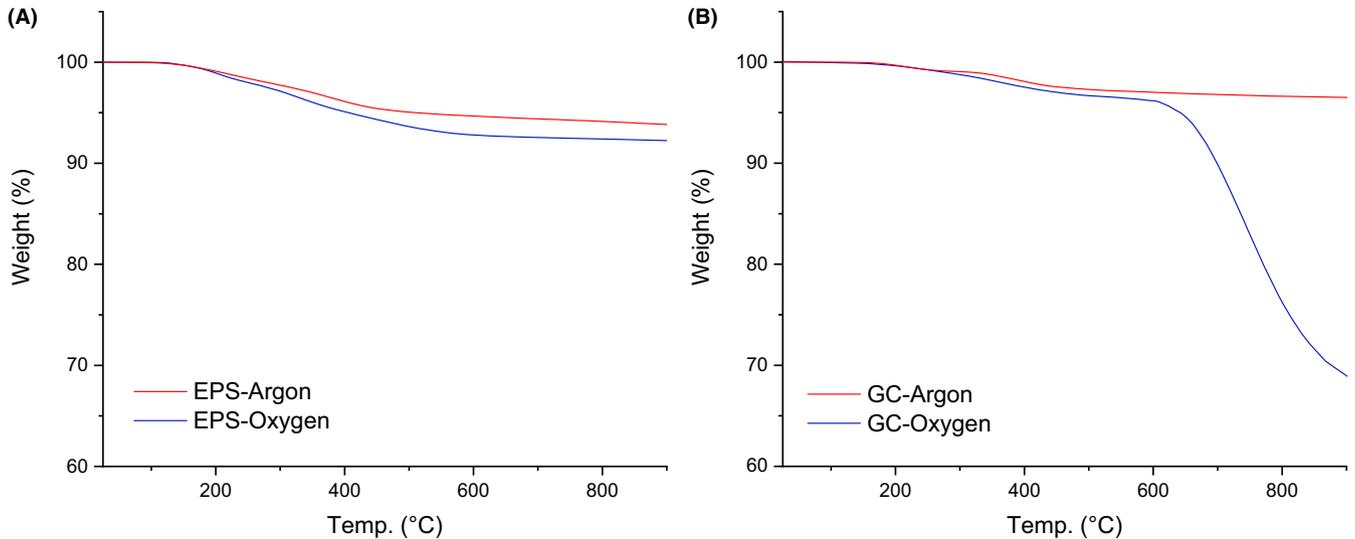
FIGURE 3 Weight loss of the alumina foams under oxygen and argon for (A) EPS and (B) GC. Volume addition of pore formers is 25% which represents 1.5 wt. % for EPS and 35 wt. % for GC
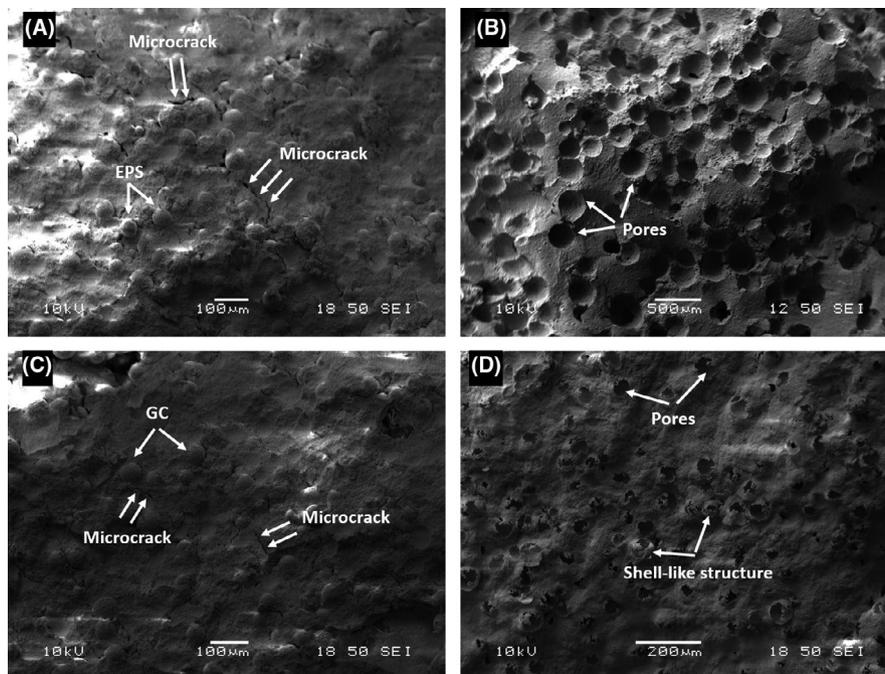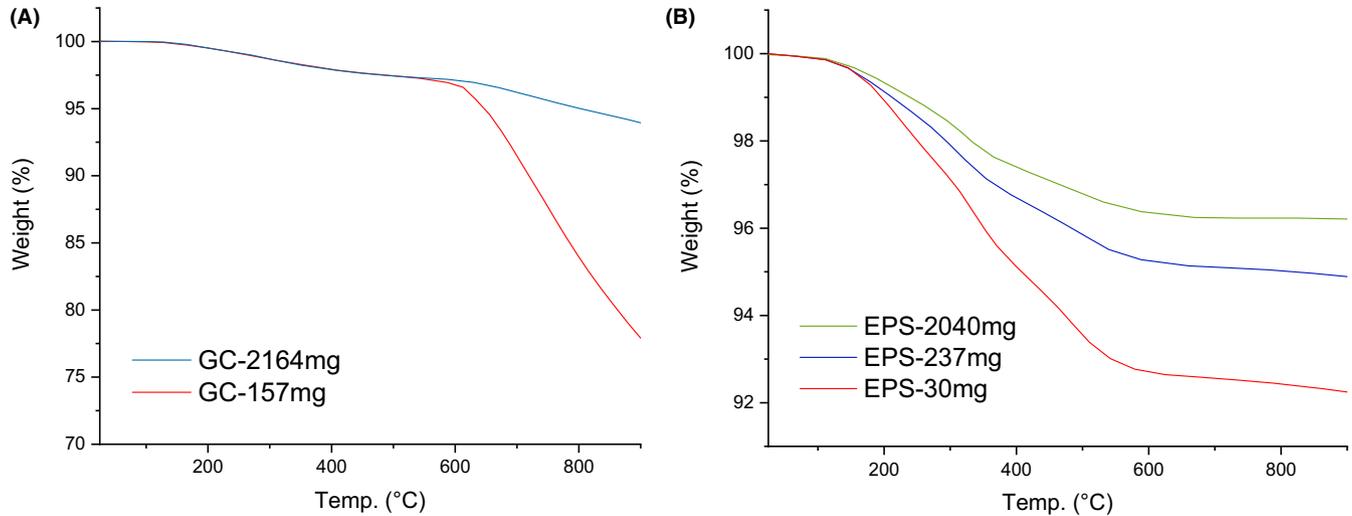

FIGURE 4 Morphology of the cross-section of the alumina ceramic body (A) before EPS burnout, (B) after EPS burnout under oxygen, (C) before GC burnout, and (D) after GC burnout under oxygen
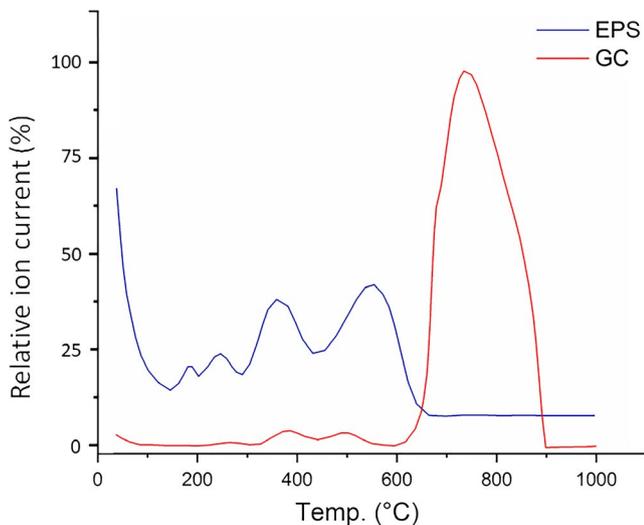
burnout procedure was the same for both templates, a thin ceramic layer formed a shell-like structure on the pores by glassy carbon (Figure 4D), probably due to the longer time and higher temperature needed for complete GC burnout. This causes the presintering of alumina powder on the surface of the GC before the (entire) GC is decomposed.

The effect of specimen size on the burnout cycle is important especially for industries, where large samples with complex shapes are manufactured. The burnout of the sacrificial template from different sizes of alumina bodies is shown in Figure 5.

As can be concluded from the graphs, the decomposition of the organics and the escape of the evolved gases take a longer time for the thicker sample than the thinner one. During the burnout, the oxygen accelerated the decomposition of organics first at the surface releasing carbon dioxide. Then, the air penetrated the entire (body) of the sample replacing the volatiles. As more oxygen penetrates inside the porous ceramic body, more organics decompose. With the increasing size of the samples, more time is required for the volatiles to diffuse to the (specimen) surface. This explains the slower weight loss for bigger samples. The effect is pronounced

(A)

(B)

FIGURE 5   Effect of size on the weight loss during the burnout process under oxygen for (A) GC and (B) EPS

FIGURE 6   The release of carbon dioxide during the EPS burnout and the GC burnout using mass spectroscopy attached to the TGA

Figure 6 shows the release of carbon dioxide during the EPS and the GC burnout measured by mass spectroscopy. As both templates used were organics, it was expected to form carbon dioxide or carbon monoxide during the burnout. As shown in Figure 6, the peaks for CO_2 released for EPS burnout are below 600°C, while the release of CO_2 during GC burnout is in the temperature range of 600-900°C, and it is 20 times higher than the one during EPS burnout. The amount of CO_2 released during burnout can strongly affect the mechanical properties of the ceramic foams.

Ceramics are strong and brittle related to their compressive strength and tensile strength, respectively. Compared to other materials like metals, ceramics are known to have good compressive strength due to its predominant ionic nature bonding which acts as a resistance to the movement of defects such as cracks. However, the number and the size of the defects influence on the compressive strength. During the pyrolysis step, the released gases were accelerated by increasing the heating rate. If the rate of formation of this volatiles is higher than their escape out rate, the internal stress increases and creates defects like microcracks and bloating that act as stress concentration sites on loading and lead to failure at lower applied stress. The comparison of the compressive strength of alumina ceramics containing GC and EPS, burnout conducted at different heating rates of 1, 3, and 10°C/min, with deviations of 0.35 MPa for GC and 0.2 MPa for EPS, is reported in Table 1. It can be concluded that the compressive strength of porous ceramics for both GC and EPS decreases rapidly by increasing the heating rate.

The compressive strength of alumina-EPS was affected by factors such as the expansion of EPS during gelation, the mismatch in thermal expansion coefficients (CTE) between EPS and alumina, bubble formation during EPS burnout, the buildup of internal stress during the fast burnout cycle, and so on. Besides the mentioned factors for EPS,

when GC was used as the sacrificial template. It can be seen in Figure 5A that the glassy carbon removal starts when the temperature increases above 600°C, and with the increase in sample size, the burnout of carbon does not show a rapid decrease in mass at $T > 600$°C, confirming that the slower kinetics of the burnout process. In the case of EPS burnout, the weight loss starts around 200°C, and when it reaches 600°C, the temperature at which GC burnout starts, the weight loss curve has leveled out. However, by increasing the sample size, the weight loss is decreased same as GC, but it should be noted that the difference in weight loss for the smallest and largest samples tested here is <5 wt. % for EPS, while in the case of GC it is about 15 wt. %, which is a big advantage for EPS.

TABLE 1 Compressive strength of foams after templates burnout under oxygen at different heating rates to 600°C

	1°C/min	3°C/min	10°C/min
Alumina-GC	2.31 (MPa)	2.22 (MPa)	1.23 (MPa)
Alumina-EPS	5.18 (MPa)	4.61 (MPa)	3.21 (MPa)

the release of a large amount of volatiles and short-range temperature of glassy carbon burnout (as described earlier) affected the compressive strength of alumina-GC. This explains the lower compressive strength for the alumina-GC than alumina-EPS in all three heating rates. As can be extracted from the values in Table 1, the compressive strength for alumina-GC at 1°C/min heating rate is 55% less than the compressive strength of alumina-EPS at the same heating rate. By increasing the heating rate to 3°C/min, the compressive strength ratio is not changed notably (52%), while in the case of the heating rate of 10°C/min, the compressive strength of alumina-GC is 62% less than alumina-EPS. This shows that increasing the heating rate has a more negative effect on the specimen prepared using GC compared to the ones using EPS.

4 | CONCLUSIONS

Alumina porous ceramics using hollow pre-expanded microspheres (Expancel) and glassy carbon microspheres were successfully prepared by the gel-casting technique. The furnace atmosphere strongly affected the burnout process and showed a higher weight decrease for the specimens which were burned out under oxygen compared to the ones under Argon. Because in the inert atmosphere only thermal decomposition took place, while in the presence of oxygen both combustion and decomposition were involved in the burnout cycle. Moreover, decomposition and volatile removal were influenced by the sample size, as by increasing the size the volatile removal decreased for both Expancel and glassy carbon. The mechanical properties showed that the compressive strength of the foams prepared by using the glassy carbon was lower than the ones using Expancel. Because the 20 times higher amount of released gases for glassy carbon increased the internal stress and caused some defects like microcracks and bloating to be formed, which consequently led to failure at lower stress. Moreover, the compressive strength of porous ceramics for both glassy carbon and Expancel was decreased rapidly by increasing the heating rate, since the rate of formation of the volatiles was higher than the escape out rate. It can be concluded that using Expancel as the sacrificial template is a promising template to be used in industries to manufacture porous ceramics in large sizes and scales, since saving time and energy is very important.

ORCID

Farid Akhtar https://orcid.org/0000-0003-4888-6237

REFERENCES

1. Colombo P. Conventional and novel processing methods for cellular ceramics. Philos Trans A Math Phys Eng Sci. 2006;364:109–24.
2. Studart AR, Gonzenbach UT, Tervoort E, Gauckler LJ. Processing routes to macroporous ceramics: A review. J Am Ceram Soc. 2006;89:1771–89.
3. Hammel EC, Ighodaro OL, Okoli OI. Processing and properties of advanced porous ceramics: An application based review. Ceram Int. 2014;40:15351–70.
4. Sarkar N, Kim IJ. Porous ceramics In: Mohamed A., editor. Advanced Ceramic Processing. Rijeka: InTech, 2015; p. 55–8.
5. Ishizaki K, Komarneni S, Nanko M. Applications of porous materials In: Ishizaki K, Komarneni S, Nanko S, editors. Porous Materials: Process Technology and Applications. Boston, MA: Springer; 1998:181–201.
6. Saggio-Woyansky J, Scott CE, Minnear WP. Processing of porous ceramics. Am Ceram Soc Bull. 1992;71:1674–82.
7. Zhang W, Wang H, Jin Z. Gel casting and properties of porous silicon carbide/silicon nitride composite ceramics. Mater Lett. 2005;59:250–6.
8. Gauckler LJ, Graule T, Baader F. Ceramic forming using enzyme catalyzed reactions. Mater Chem and Phys. 1999;61:78–102.
9. Yang J, Yu J, Huang Y. Recent developments in gelcasting of ceramics. J Eur Ceram Soc. 2011;31:2569–91.
10. Young AC, Omatete OO, Janney MA, Menchhofer PA. Gelcasting of alumina. J Am Ceram Soc. 1991;74:612–8.
11. Janney MA, Omatete OO, Walls CA, Nunn SD, Ogle RJ, Westmoreland G. Development of low-toxicity gelcasting systems. J Am Ceram Soc. 1998;81:581–91.
12. Sun Y, Shimai S, Peng X, Dong M, Kamiya H, Wang S. A method for gelcasting high-strength alumina ceramics with low shrinkage. J Mater Res. 2014;29:247–51.
13. Ohji T, Fukushima M. Macro-porous ceramics: processing and properties. Int Mat Rev. 2012;57:115–31.
14. Santa Cruz H, Spino J, Grathwohl G. Nanocrystalline ZrO2 ceramics with idealized macropores. J Eur Ceram Soc. 2008;28:1783–91.
15. Ciurans Oset M, Nordin J, Akhtar F. Processing of macroporous alumina ceramics using pre-expanded polymer microspheres as sacrificial template. Ceram. 2018;1:329–42.
16. Andersson L, Bergström L. Gas-filled microspheres as an expandable sacrificial template for direct casting of complex-shaped macroporous ceramics. J Eur Ceram Soc. 2008;28:2815–21.

17. Topateş G, Petasch U, Adler J, Kara F, Mandal H. Production and permeability of porous Si3N4 ceramics produced by starch addition. J Asian Ceram Soc. 2013;1:257–61.

18. Ding S, Zeng Y, Jiang D. In-situ reaction bonding of porous SiC ceramics. Mater Char. 2008;59:140–3.

19. Mallick D, Das S, Chakrabarti OP, Maiti HS, Majumdar R. Cellular porous SiC ceramics derived from Indian dicotyledonous woods and their application potential as hot gas filtration materials. Adv Appl Ceram. 2006;105:246–52.

20. Roy S, Schell KG, Bucharsky EC, Hettich P, Dietrich S, Weidenmann KA, et al. Processing and elastic property characterization of porous SiC preform for interpenetrating metal/ceramic composites. J Amer Ceram Soc. 2012;95:3078–83.

21. Sharifi L, Ghanbarnezhad S, Ghofrani S, Mirhosseini SH. High porous alumina bodies: production and properties via gel-casting technique. Int J Adv Sci Technol. 2014;65:59–70.

22. Guo X. Gel Casting of High Strength Ceramics (unpublished dissertation). Gothenburg: Chalmers University of Technology; 2011.